Leakage Current Suppression and Ripple Power Reduction for Transformer-less Single-Phase Photovoltaic Inverters

Xin Li
School of Information Science and Engineering
Central South University
ChangSha, China
lixincsu@csu.edu.cn

Zhongting Tang
School of Information Science and Engineering
Central South University
ChangSha, China
tinatcsu@163.com

Mei Su
School of Information Science and Engineering
Central South University
ChangSha, China
sumeicsu@mail.csu.edu.cn

Qi Zhu
School of Information Science and Engineering
Central South University
ChangSha, China
csu_zhuqi@163.com

Yonglu Liu
School of Information Science and Engineering
Central South University
ChangSha, China
liuyonglu@csu.edu.cn

Yao Sun
School of Information Science and Engineering
Central South University
ChangSha, China
yaosuncsu@gmail.com

***Abstract*—Transformer-less single-phase grid-tied inverter is attractive due to low cost, high efficiency, and small size. However, leakage current and second-order ripple power have to be well dealt with. Because the leakage current is a potential threat for body safety and the ripple power will decrease overall efficiency and system reliability. Both issues become obstacles for practical applications. This paper proposes a method to achieve leakage current suppression and ripple power reduce simultaneously. The main circuit is formed by adding an extra arm and a decoupling capacitor to the traditional single-phase voltage source inverter. The additional arm is controlled to keep the common voltage constant and divert the ripple power to the decoupling capacitor. A decoupled control method is also developed to achieve independent control of power factor correction and power decoupling. Finally, simulation results are presented to show the effectiveness.**

Keywords—leakage current; decoupling; common mode voltages; ripple power

I. INTRODUCTION (*HEADING 1*)

Photovoltaic (PV) is one of the most promising renewable energy sources. Because the energy processed by PV system comes from the sun, which is free and available almost everywhere. It is predicted to be up to 60% of the total energy by the end of this century [1]. Grid-tied inverter plays a critical role in PV systems because the reliability, power density, efficiency and quality of power are closely related to it. Transformer-less inverters have been widely used as interfaces due to low cost, high efficiency, and small size compared with the ones with transformer [2]. Unipolar sinusoidal pulse width modulation (SPWM) is preferred compared with bipolar SPWM due to smaller filter inductance requirement, higher efficiency and higher grid-connected current quality. However, the common characteristics under unipolar SPWM are poor [3]. The caused high common mode voltage forces common current, which should be limited for human safety and EMI compatibility [4, 5]. According to German Standard DIN VDE 0126-1-1, the RMS of the earth leakage current should be limited under 300mA [6]. To deal with pulsed common mode voltages, a variety of modified full H-bridge inverters are proposed [2, 7]. They can be divided into two categories: zero-state decouple topologies, zero-state mid-point clamped topologies and solidity clamped topologies.

On the other hand, the second-order ripple power, which is inherent in single-phase system, is also troublesome. The power flowing to the grid is time varying at twice the grid frequency, while the power extracted from the PV panel is constant for maximizing energy harvest. Consequently, large aluminum electrolytic capacitors (AECs) have to be employed to buffer the power mismatch between the grid and the PV source. However, AECs are featured as a lifetime limited component. And it is reported that most inverter failures are blamed on AECs [9]. To improve system reliability, a lot of active power decouple methods have been proposed recently

This work was supported by the National Natural Science Foundation of China under Grant 51677195 and 2016JJ1019, the Fundamental Research Funds for the Central Universities of Central South University.

for PV applications [9, 10]. The basic idea is to divert the second ripple power to an extra small energy storage component with long lifetime. Then the dc-link capacitor in inverters can be replaced with small film capacitors.

This paper introduces a topology with both leakage current suppression and ripple power reduce capabilities. Different from the topologies above, the leakage current suppression is achieved by the design of modulation schemes. The operation principle is firstly introduced in detail. Then a decoupled control method is developed to achieve independent control of the grid current and power decouple. Finally, the proposed method is verified by simulations results.

II. CIRCUIT CONFIGURATION AND OPERATION PRINCIPLE

A. Circuit Configuration

Fig. 1(a) shows the main circuit topology, which will be researched in this paper. Similar to four-leg transformerless three-phase inverter proposed in [13, 14], it is formed by adding an extra bridge arm, a filter L_3, and a decoupling capacitor C_d to a voltage source H-bridge inverter. Note that this topology is identical to that proposed in [15], and thereafter the modulation strategy for minimizing the capacitor C_d is studied in [16]. However, in both of them the study emphasis is focused on the ripple power decouple function. Besides that, theleakage current suppression function is also investigated in this paper.

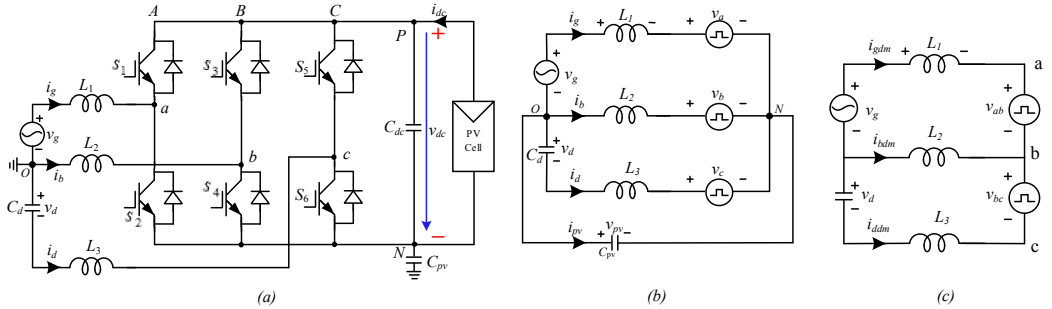

Fig. 1. (a) Main circuit topology. (b) Equivalent circuit with considering common voltage. (c) Equivalent circuit with only differential voltage.

B. Operation Principle

As the principle of decoupling ripple power is well explained in [15,16], the principle of leakage current suppression will be introduced in detail in this section. The equivalent circuit with considering common voltage is shown in Fig. 1(b). v_a, v_b, and v_c are the voltages between the mid-points a, b, and c of the bridge-legs and the reference terminal N. The common voltage is defined as:

$$v_{cm} = \frac{v_a + v_b + v_c}{3} \tag{1}$$

Applying Kirchhoff laws, the following mathematical equations can be obtained.

$$v_{pv} = si_g L_1 + v_a - v_g \tag{2}$$

$$v_{pv} = si_b L_2 + v_b \tag{3}$$

$$v_{pv} = si_d L_3 + v_d + v_c \tag{4}$$

$$i_g + i_b + i_c + i_{pv} = 0 \tag{5}$$

where s represents the differential operator. The leakage current is given by:

$$i_{pv} = sv_{pv} C_{pv} \tag{6}$$

where C_{pv} is the value of parasitic capacitor. It varies with the material and size of the solar array, ambient temperature, humidity, dust, and other environmental conditions. And usually it is small with a value of dozens to hundreds of nanofarad.

Assume L_1=L_2=L_3=L, according to (2)-(6), the leakage current i_{pv} can be rewritten as:

$$\begin{aligned} i_{pv} &= G(s)\left[\frac{(v_a+v_b+v_c)}{3} + \frac{v_d - v_g}{3}\right] \\ G(s) &= \frac{sC_{pv}}{s^2 LC_{pv}/3+1} \end{aligned} \tag{7}$$

To make the leakage current i_{pv} small enough to meet the Standard DIN VDE 0126-1-1, v_{pv} should be kept varying with low frequency. As v_g and v_d vary with the grid frequency, then, high frequency components should not be involved in v_{cm}. And usually v_{cm} is kept constant.

III. MODULATION STRATEGY

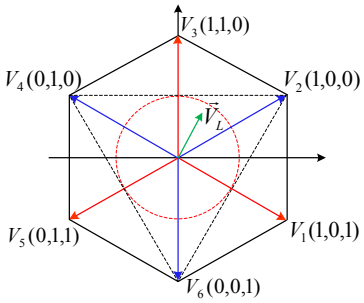

Fig. 2. Space vector for three-phase voltage source converter.

Fig. 2 shows the classic space vector modulation diagram. To keep the common voltage v_{cm} constant, only the active sectors (V_1, V_3, V_5) or (V_2, V_4, V_6) are employed to synthesize the desired voltages. When V_1, V_3 and V_5 are adopted, the common voltage is $2u_{dc}/3$; when V_2, V_4 and V_6 are adopted, the resulted common voltage is $u_{dc}/3$.

In this paper, the set of active sectors (V_2, V_4, V_6) is used for a smaller common voltage. However, the desired voltage vector must lie in the inscribed circle in Fig. 2, which decreases the dc-link voltage utilization.

Assume the desired line-line voltages v_{ab} and v_{bc} are known. Then the duty ratios can be obtained by solving the following equations:

$$\begin{cases} d_2 v_{dc} + d_4 v_{dc} = v_{ab} \\ d_4 v_{dc} + d_6 v_{dc} = v_{bc} \\ d_2 + d_4 + d_6 = 1 \end{cases} \tag{8}$$

where d_2, d_4, and d_6 are duty ratios of V_2, V_4, and V_6. They can be expressed as

$$\begin{cases} d_2 = \left(1 + 2\frac{v_{ab}}{v_{dc}} + \frac{v_{bc}}{v_{dc}}\right)/3 \\ d_4 = \left(1 - \frac{v_{ab}}{v_{dc}} + \frac{v_{bc}}{v_{dc}}\right)/3 \\ d_6 = \left(1 - \frac{v_{ab}}{v_{dc}} - 2\frac{v_{bc}}{v_{dc}}\right)/3 \end{cases} \tag{9}$$

IV. CONTROLLER DESIGN

When designing the controller, only the differential-mode circuit is taken into account. v_{ab} and v_{bc} are the control variables. i_{gdm}, i_{bdm}, and i_{ddm} are differential-mode currents. The equivalent circuit is shown in Fig. 1(c). According to the Kirchhoff laws, the following differential equations are derived:

$$L\frac{di_{gdm}}{dt} = v_g + L\frac{di_{bdm}}{dt} - v_{ab} \tag{10}$$

$$L\frac{di_{ddm}}{dt} = L\frac{di_{bdm}}{dt} + v_{bc} - v_d \tag{11}$$

$$C_d\frac{dv_d}{dt} = i_{ddm} \tag{12}$$

$$i_{gdm} + i_{bdm} + i_{ddm} = 0 \tag{13}$$

Substitute (13) into (10) and (11), yields:

$$\begin{pmatrix} L\frac{di_{gdm}}{dt} \\ L\frac{di_{ddm}}{dt} \end{pmatrix} = \begin{pmatrix} u_1 \\ u_2 \end{pmatrix} = \begin{pmatrix} -\frac{2}{3L} & -\frac{1}{3L} \\ \frac{1}{3L} & \frac{2}{3L} \end{pmatrix} \begin{pmatrix} v_{ab} \\ v_{bc} \end{pmatrix} + \begin{pmatrix} \frac{2}{3L}v_g + \frac{v_d}{3L} \\ \frac{-v_g}{3L} - \frac{2v_d}{3L} \end{pmatrix} \tag{14}$$

According to the control objectives, the references i_{gdm} and i_{ddm} can be obtained as shown in Fig. 3. Then the following tasks become the design of current controllers. According to the property of the current references, two proportional resonant controllers are used in this paper. And the output of the first proportional resonant controller PR1 is u_1 and the output of the second proportional resonant controller PR2 is u_2. Then references for v_{ab} and v_{bc} are

$$\begin{pmatrix} v_{ab} \\ v_{bc} \end{pmatrix} = \begin{pmatrix} -\frac{2}{3L} & -\frac{1}{3L} \\ \frac{1}{3L} & \frac{2}{3L} \end{pmatrix}^{-1} \begin{pmatrix} u_1 - \frac{2}{3L}v_g - \frac{v_d}{3L} \\ u_2 + \frac{v_g}{3L} + \frac{2v_d}{3L} \end{pmatrix} \tag{15}$$

With the designed feed-forward decoupling controller the input current control and power decoupling control are fully decoupled.

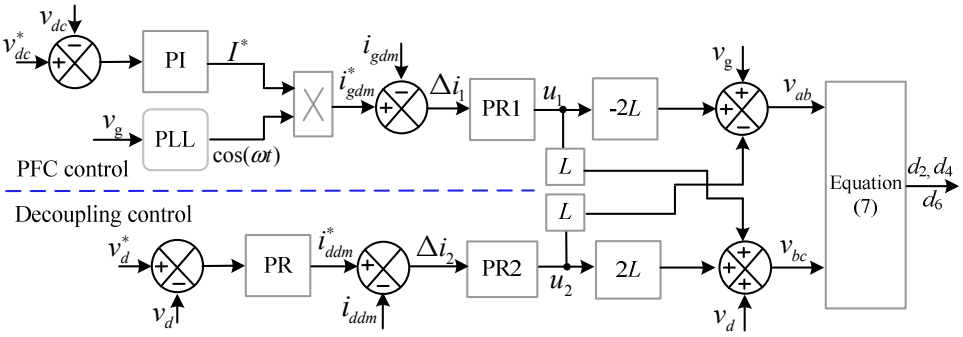

Fig. 3. Block diagram of the control scheme

V. SIMULATION RESULTS

To verify the proposed method, numerical simulations are performed on MATLAB/simulink platform. The main parameters are as follows: $V=110V$, $v_{dc}=200V$, $\omega=314rad/s$, $L_1=L_2=L_3=3mH$, $C_{dc}=30uF$, $C_d=150\mu F$, $C_{pv}=100nF$, switching frequency $f_s=20kHz$.

Fig. 4(a) shows the steady-state operation waveforms of grid voltage/current, and dc-link voltage/current. As can be observed, second order ripple doesn't appear in the dc-link

voltage as the ripple power is diverted to the decoupling capacitor C_d.

Fig. 4(b) shows the simulation results of the decoupling capacitor voltage/current, common-mode voltage and the leakage current with the proposed method. It can be founded that the decoupling capacitor voltage varies with the grid frequency as results of buffering the ripple power. v_{pv} varies with grid frequency. Therefore, the leakage current is small. And the RMS of the leakage current is only *48mA*, which meets the standard.

Fig. 4(c) shows the simulation waveforms of common-mode voltage and the leakage current when adopting the modulation strategy in [11]. As can be seen, v_{pv} contains lots of high frequency components and the RMS of the leakage current i_{pv} is up to *1.25A*. That indicates the effectiveness of the proposed method on leakage current suppression.

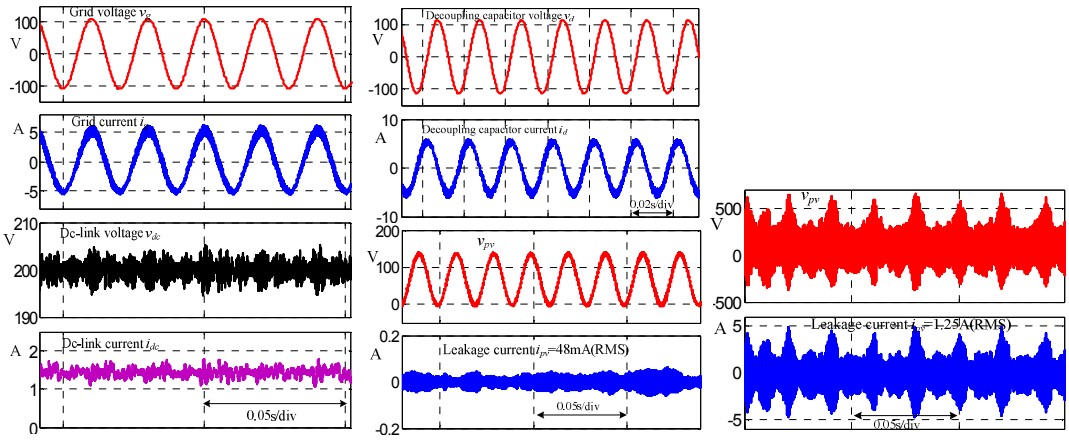

(a) (b) (c)

Fig. 4. Steady-state simulation waveforms. (a) Grid voltage, grid current, dc-link voltage and dc-link current.(b). Decoupling capacitor voltage/current, common-mode voltage and the leakage current with the proposed method. (c) Common-mode voltage and the leakage current when adopting the modulation strategy in [11].

VI. CONCLUSION

In this study, the proposed modulation strategy has realized leakage current suppression and ripple power reduction for transformer-less single-phase photovoltaic inverters. Then, only a small dc-link capacitor is required and the leakage current was reduced. To achieve easy control, a decoupled control method is developed. Simulation results verify the effectiveness of the proposed modulation strategy and control method.

REFERENCES

[1] Z. Zhao, High efficiency single-stage grid-tied PV inverter for renewable energy system. (PhD). United States: Virginia Polytechnic Institute and State University, Blacksburg; 2012 (VA 24061).

[2] M. Islam, S. Mekhilef, and M. Hasan, "Single phase transformerless inverter topologies for grid-tied photovoltaic system: A review," Renewable and Sustainable Energy Reviews, vol. 45, pp. 69-86, 2015.

[3] H. Xiao and S. Xie, "Leakage current analytical model and application in single-phase transformerless photovoltaic grid-connected inverter," IEEE Trans. Electromagn. Compat., vol. 52, no. 4, pp. 902–913, Nov. 2010

[4] R. Araneo, S. Lammens, M. Grossi, and S. Bertone, "EMC issues in highpower grid-connected photovoltaic plants," IEEE Trans. Electromagn. Compat., vol. 51, no. 3, pp. 639–648, Aug. 2009.

[5] H. Xiao, S. Xie, Y. Chen, and R. Huang, "An optimized transformerless photovoltaic grid-connected inverter," IEEE Trans. Ind. Electron., vol. 58, no. 5, pp. 1887–1895, May 2011.

[6] Automatic Disconnection Device Between a Generator and the Public Low-Voltage Grid, DIN VDE V 0126-1-1, 2006.

[7] W. Li, Y. Gu, H. Luo, W. Cui, X. He, and C. Xia, "Topology review and derivation methodology of single-phase transformerless photovoltaic inverters for leakage current suppression, " IEEE Trans. Ind. Electron., vol. 62, no. 7, pp. 4537–4551, Jul. 2015.

[8] A. Ristow, M. Begovic, A. Pregelj, and A. Rohatgi, "Development of a methodology for improving photovoltaic inverter reliability," IEEE Trans. Ind. Electron., vol. 55, no. 7, pp. 2581–2592, Jul. 2008

[9] H. Hu, S. Harb, N. Kutkut, L.Batarseh, and Z. J. Shen, "A review of power decoupling techniques for microinverters with three different decoupling capacitor locations in PV systems," IEEE Trans. Power Electron, vol. 28, no. 6, pp. 2711-2726, Jun, 2013.

[10] Y. Sun, Y. Liu, M. Su, W. Xiong, and J. Yang, "Review of Active Power Decoupling Topologies in Single-Phase Systems," IEEE Trans. Power Electron., in press.

[11] Y. Tang, W. Yao, P.C. Loh, and F. Blaabjerg, "Highly reliable transformerless photovoltaic inverters with leakage current and pulsating power elimination," IEEE Trans. Ind. Electron., in press.

[12] W. Qi,, H. Wang, X. Tan, et al., "A novel active power decoupling single-phase PWM rectifier topology," in Proc. IEEE APEC, Fort Worth, TX, 2014. vol. 3, pp. 89-95.

[13] A. Julian, T. Lipo, and G. Oriti, "Elimination of common-mode voltage in three-phase sinusoidal power converters," IEEE Trans. Power Electron., vol. 14, no. 5, pp. 982–989, Sep. 1999.

[14] X. Guo, R.He , J. Jian, Z. Lu, X. Sun, and J. Guerrero, "Leakage Current Elimination of Four-Leg Inverter for Transformerless Three-Phase PV Systems," IEEE Trans. Power Electron., in press.

[15] H. Li, K. Zhang, H. Zhao, S. Fan, and J. Xiong, "Active power decoupling for high-power single-phase PWM rectifiers," IEEE Trans. Power Electron., vol. 28, no. 3, pp. 1308-1319, Mar, 2013.

[16] H. Wu, S. C. Wong, and C. Tse, "Control and Modulation of Bidirectional Single-Phase AC-DC Three-phase-leg SPWM Converters with Active Power Decoupling for a Minimal Storage Capacitance," IEEE Trans. Power Electron., in press.